



ISSN: 0067-2904

Medical Ultrasound Image Quality Enhancement and Regions Segmentation

Ayat Ali Al-jaburi *, Ahlam Hanoon AL-sudani

Computer Eng. Department, College of Engineering, University of Baghdad, Baghdad, Iraq

Received: 2/7/2021

Accepted: 14/1/2022

Published: 30/10/2022

Abstract

Medical Ultrasound (US) has many features that make it widely used in the world. These features are safety, availability and low cost. However, despite these features, the ultrasound suffers from problems. These problems are speckle noise and artifacts. In this paper, a new method is proposed to improve US images by removing speckle noise and reducing artifacts to enhance the contrast of the image. The proposed method involves algorithms for image preprocessing and segmentation. A median filter is used to smooth the image in the pre-processing. Additionally, to obtain best results, applying median filter with different kernel values. We take the better output of the median filter and feed it into the Gaussian filter, which then feeds the output of the Gaussian filter into histogram equalization to improve image visualization. The segmentation is done by thresholding and region growing segmentation. The value of threshold 128 was found to be better after we tested many values of thresholding. This value of thresholding combined with region growing gave accurate result segmentation of images. This paper demonstrates how image noise, artifacts and techniques were used effectively to improve image quality, and the analysis of performance of various techniques.

Keywords: US, Speckle noise, Artifact, Thresholding, Region Growing, Segmentation.

تحسين جودة وتجزئة صور الموجات فوق الصوتية الطبية

اياات علي الجبوري *, احلام حنون السوداني

كلية الهندسة، قسم هندسة الحاسبات، جامعة بغداد، بغداد، العراق.

الخلاصة

تميز الموجات فوق الصوتية الطبية (US) بالعديد من الميزات التي تجعلها تستخدم على نطاق واسع في العالم. هذه الميزات هي الأمان والتوافر والتكلفة المنخفضة. ومع ذلك، مع هذه الميزات، فإن الموجات فوق الصوتية تعاني من العديد من المشاكل. هذه المشاكل هي (Speckle noise and Artifact). لقد طورنا طريقة جديدة لتحسين صورة US عن طريق إزالة (speckle noise and artifact) لتحسين جودة الصورة وتعزيز تباين الصور. خطوات هذه الطريقة هي خوارزميات المعالجة المسبقة (Preprocessing) والتجزئة (Segmentation). تم استخدام مرشح (Median) لتنعيم الصورة للمعالجة المسبقة. أفضل أداء لهذا المرشح هو إدخال مرشح (Gaussian) وإخراج هذا المرشح هو إدخال معادلة الرسم

*Email: ayata8179@gmail.com

البياني (Histogram) لتحسين تصور الصورة. . تم إجراء التجزئة عن طريق تجزئة العتبة (Thresholding) والمنطقة المتزايدة (Region Growing). قيمة العتبة هي 128 بعد التجربة لعدد من القيم كان الاستنتاج نظريا ان 128 افضل قيمة مجتمعة مع المنطقة المتزايدة لإعطاء نتائج دقيقة لتجزئة الصور. توضح هذه الورقة (artifact, speckle noise) والتقنيات المستخدمة بشكل فعال لتحسين جودة الصورة ويتم تحليل أداء التقنيات المختلفة بموضوعية. (Objectively)

1. Introduction

Ultrasound (US) medical imaging, due to its many advantages, is one of the most commonly applied methods today. It consists of a mechanical length wave using a frequency that exceeds the top limits of the human auditory system [1]. The benefits of ultrasound include safety, low costs, non-invasiveness and in-pocket portability, which have made it an advantageous tool for showing accurate information about medical soft tissue [2].

However, these benefits of ultrasound suffer from speckle noise and artifact effects of diagnostic. Besides, due to the presence of speckles in ultrasound images, the enhancement of US image is extremely difficult especially in images of the liver and the kidney whose underlying structures are too small to be resolved by large wavelength [3]. They also complicate further image processing, such as image segmentation [4]. Thus, before making any image analysis, suppressing the speckle noise and enhancing the image without losing valuable image features is a very vital step. The median filtering technique smooth the image but does not enhance the edge, whereas Gaussian filtering technique smooth the image in the whole but at the same time the image become blurred. For that we used histogram equalization technique to increase the intensity of the image and the kidney edge is clearer compared to the original image. Therefore, before the segmentation process, enhancement of the image using median filtering, Gaussian filter and histogram equalization can be performed for a better segmentation result.

In this paper, Thresholding and region growing segmentation methods are applied to achieve more accurate results.

2. Ultrasonic Image Artifacts

Although the technological progress in the diagnostic ultrasound equipment is very important, artifacts remain the diagnostic challenge for the sonographers. Artifacts may be described as echoes shown in images that do not reflect the real picture of patients in their intensity or location [5]. These artifacts have an effect on image quality. They can be classified into three groups: attenuation artifacts, wave propagation artifacts and sound of speed artifacts[6].

2.1 Attenuation Artifacts

❖ Shadowing artifact: - appear when scanning with tissue or further objects, metal instruments like bone that create shadow areas in the images of US as shown in Figure 1. These results from the transmission of those sound waves across the front and back surfaces of an instrument and these waves do not have enough intensity to reflect the tissue and pass back through the instrument to arrive to the probe. In other words, the US beam absorption via a dense body in its straight route produces a region of darkness on the screen [7].



Figure 1: Shadowing artifacts (white arrow) [8].

❖ Enhancement artifact:- This kind appears due to hyper intensive signal, which appears as soon as a very low attenuation happens distal to the transducer, It comes into view as a brighter than natural image area [9] as in shown in Figure 2.

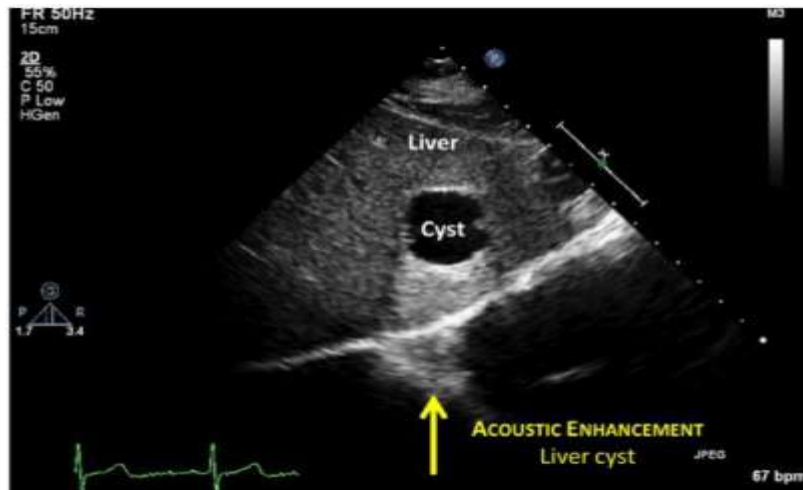


Figure 2: Enhancement artifact (yellow arrow) [10]

2.2 Wave Propagation Artifacts

❖ Comet-tail: - Is a type of the reverberation artifact, appears as dense tapering trail of echoes just distal to a robustly reflecting structure [7] as in shown in Figure 3.

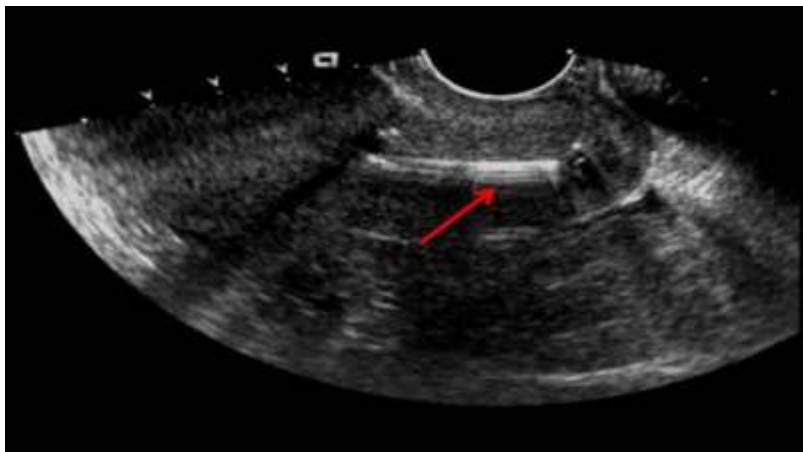


Figure 3: Comet –Tail artifact (red arrow) [11]

❖ Reverberation artifact: - It occurs when there is a back and forth reflection for the US energy between two interfaces throughout the acquisition of the signal and prior to the following transmitted pulse [8]. Figure 4 shows the reverberation artifact in the anterior portion of the urinary bladder (red arrow).



Figure 4: Reverberation artifact [11]

❖ Mirror image artifact: - Is uncommon but significant and appears most often as soon as probing tissues close to the pericardium or diaphragm because of reflection errors of these compact structures where a mirror image of any tissue can be seen on another side of a specular reflector [12]. As in shown in Figure 5, longitudinal US image of the liver in a 44-year-old man where a mirror image artifact (arrow) of a hepatic hemangioma that developed through the diaphragm within the lung [13].

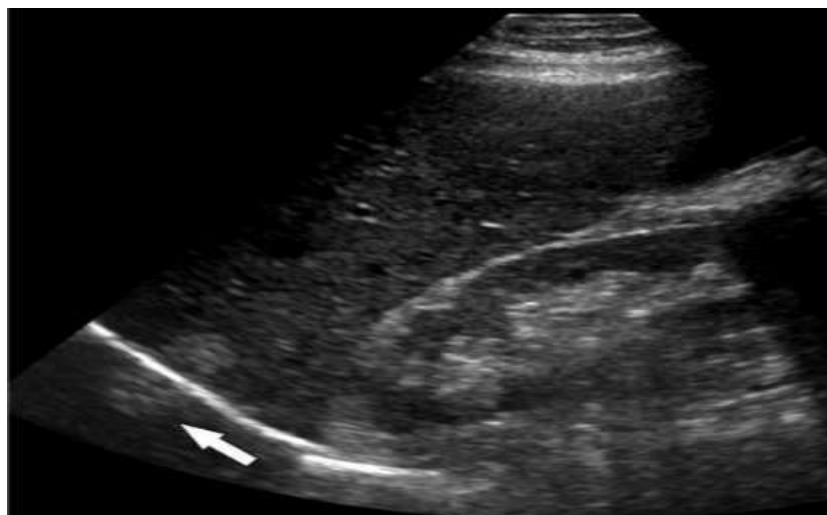


Figure 5: Mirror image(white arrow) [11]

2.3 Sound of Speed Artifacts

❖ An ultrasound machine presumes that the speed of sound is constant within the organic tissue, but sound velocities are totally different in organic tissues. When scanning an area with tissues at various speeds, far from the lower speed tissue, the incorrect depth assignment can be seen. Quick and smooth structures are often behind this artifact, observed as a cause.

Echo's that move through lesions reach the transducer a little late and in deep positions, they will be assigned creating a rupture in structures on the back [5].

❖ **Refraction artifact:** Violates the assumptions that the path of the ultrasound wave is straight and that the speed of the ultrasound wave is uniform. In this scenario, instead of the ultrasound wave traveling directly to the cardiac object and back to the transducer, the wave encounters a structure that acts as a wave refractor. This structure behaves as a lens. As the wave goes through the structure, the path of the wave is bent at the interface, and the speed of the wave is changed depending on material of the structure. This results in duplication (often partial) of the cardiac object that appears as a sort of ghost image to the side of the true image as in shown in Figure 6. The produced image is similar to that of the mirror image artifact, but it appears next to instead of underneath the true image. Common inducers of refraction artifacts are costal cartilage, fascial structures and fat, and pleural and pericardial surfaces [10].

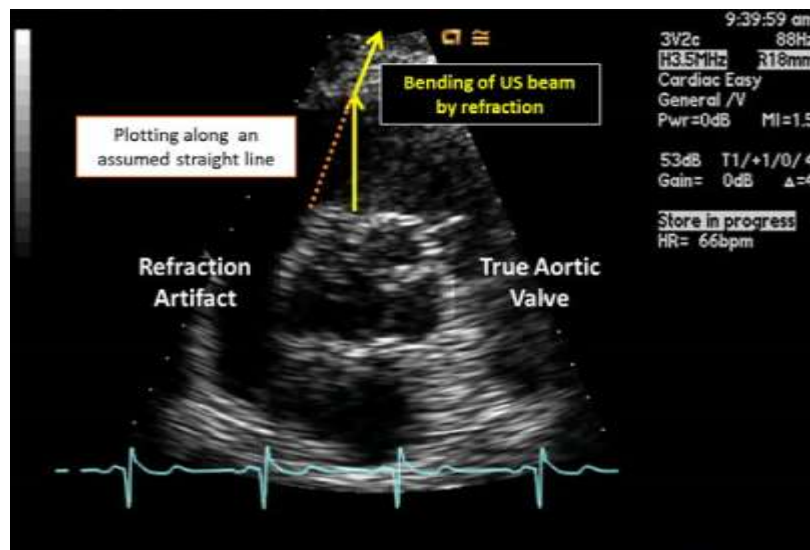


Figure 6: Refraction artifact [10]

3. Noise Model

Capturing instrument, media for data transmission, quantization of images and a discrete source of radiation are affected by image modelization. In natural images Gaussian noise (random additive) is seen [14]. Ultrasound images are mostly affected by speckling noise. As in shown in Figure 7, due to errors in data transmission. De-noise should be carried out to improve the image for such noises more precise diagnosis quality. The main aim of image-de-noise technology is removing noise of this kind while retaining important signal features as much as possible. Speckle noise is dispensed according to the gamma distribution in this Eq. (1) [15]:

$$F(g) = \left[\frac{g^{\alpha-1}}{(\alpha-1)! a^{\alpha}} e^{-\frac{g}{a}} \right] \quad (1)$$

Where α^2 is a variance that gives an idea how the pixel values are spread, α is the gamma-distribution shape parameter with range from 2.35 to 2.55, and g is the gray level.



Figure 7: Image of speckle noise [16]

4. Related Work

In recent years, researchers have achieved many successes in improving the US image, which is crucial for people working in the medical field.

For instance Nasrul Humaimi Mahmood et al. [17] Proposed an approach to obtain spleen ultrasound image and perform image quality enhancement so that the image of the spleen is clearer and easier to analyze. The used method is region of interest based image filtering. The results showed that this method can enhance the image quality especially at the region of interest specified. However, a problem may be caused due to limited mask, and the number of iterations performed in the image.

J.C. Dinis et al. [18] Proposal mainly aimed at segmenting 3D ultrasound images for fetals and making this task fast, efficient and easy. In this application, they achieved good results due to this application enabling multiple image pre-processing steps before performing a final segmentation for generating the 3D model to be manufactured by a 3D printing technique. In the case of fetus segmentation, they could not clearly distinguish the abdomen tissue of mother from fetus tissue. Especially when the tissue fetus was close to mother's abdomen walls.

Eko Supriyanto et al. [19] presented a simple guide to determine the thyroid lobes in thyroid ultrasound image. The thyroid measurement and recognition system are especially useful in medical field such as early thyroid cancer diagnostic. The thyroid ultrasound image would undergo the image enhancement method that is contrast enhancement histogram equalization to suppress speckle. Then the enhancement image would undergo local region-based active contour to segment the thyroid region. The thyroid region then is segmented into two parts that are right and left with the active contour method separately. The proposed method can be used to enhance the image and segmentation the thyroid lobe. It shows that from five samples, different people have different size of thyroid especially in measurement of width, depth and area. Research found that the right lobe is usually slightly larger than the left.

Mohammad Shorif Uddin et al. [20] Divided their work in two distinct phases: pre-processing and extraction from the candidate region. Preprocessing deals with low contrast noise and artifacts. Using the appropriate segmentation method, the kidney region is removed after noise removal. They also compare segmentation based on regions with cell segmentation. This type of method in experiment as a regional segmentation gives us better results. The experimental results show how effective the system is.

Haijiang Zhu et al. [21] A modified extraction method based on MSER (maximally stable external region) was proposed for the ultrasound segmentation of the liver lesions. This was to get stable feature regions. The method proposed used the improved MSER algorithm to save time. The performance of the proposed method was evaluated for many ultrasound images including liver lesions. The experimental results showed that the proposed method is more consistent with the regions manually extracted by medical experts. The proposed method was found to require a long time to run.

5. Materials and Methods

This experiment consists of many steps that include the collecting of 2D ultrasound kidney images, performing different image enhancements techniques, segmentation algorithms used and analysis if output image by using different parameter performance.

5.1 Test Material

The input image set is made of US digital kidney images collected from BLDEDU's Sri. B. M. Patil Medical College and Research Centre [22]. It was prepared in consultation with the medical experts from the hospital. The images in the database were captured using Phillips HD11XE US system, curvilinear transducer with frequency ranging from 5MHz to 7MHz. The sample ultrasonic medical images of kidney stones are shown in Figure 8(a) and (b).

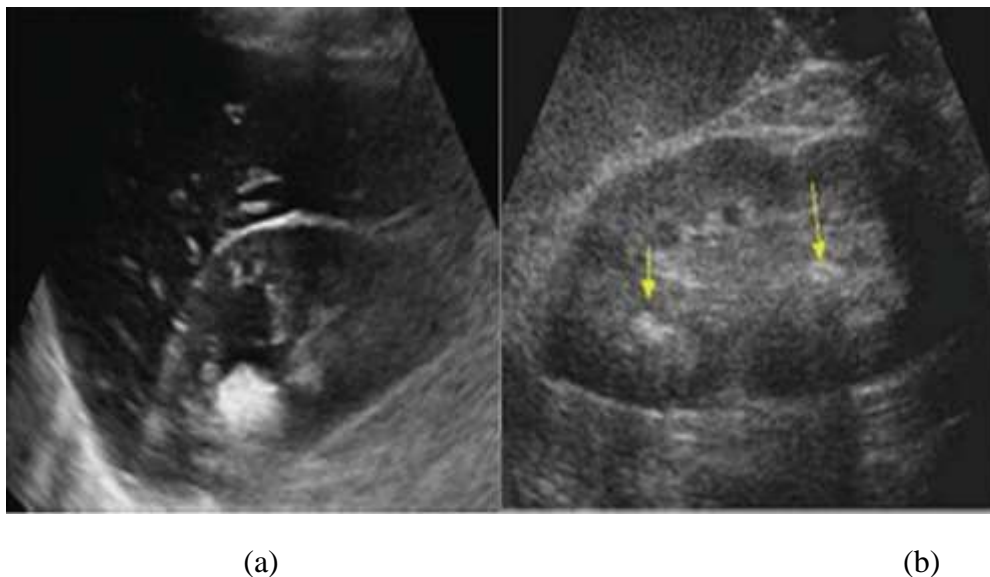


Figure 8: Sample kidney stone US images [22],(a) Sample 1 (b)Sample 2

5.2 Image Processing Algorithm

Proposed methodology involves several steps such as preprocessing, removal of speckle noise, and segmentation of preprocessed images using threshold and region growing methods to find region of interest (stone). Steps of the proposed methodology is shown in Figure 9.

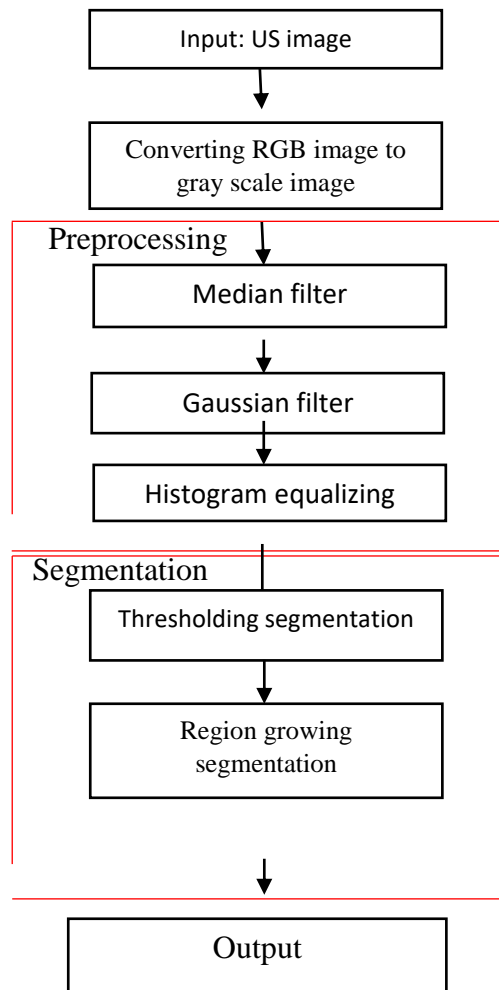


Figure 9: Flowchart of the proposed algorithm

5.3 Preprocessing

The preprocessing of images includes image filters. These filters are used to remove noise like speckle noise and reduce artifacts like shadowing to improve image quality and enhance image contrast. When using digital filters, the image is convoluted with a square matrix of size $(n * n)$ which is referred to as the kernel, where n is an odd number. Median filtering technique smooth the image but does not enhance the edge whereas Gaussian filtering technique smooth the image in the whole but at the same time the image become blurred. Thus, histogram equalization technique was used to increase the intensity of the image and for the kidney edge to become clearer compared to the original image.

5.3.1 Median filter

Median filters come with statistical filters for order-based filters. This filter work is as follows, For N observations, $X_1, X_2, X_3, \dots, X_N$ of a variant X , then the order statistics are obtained by ranking $\{X_i\}$ in ascending order as in Eq.(2)[23]:

$$X_1 \leq X_2 \leq X_3 \dots \leq X_N \quad (2)$$

The order statistics for N observations. So, an order statistics filter is an estimator $F(X_1, X_2, X_3, \dots, X_N)$.

The instruction of median filter is (3)[23]:

$$f(x, y) = \text{median} \{g(s, t)\} \quad (3)$$

$g(s, t)$: The location of this pixel.

5.3.2 Gaussian filter

This filter has Gaussian function as its impulse response. It has non uniform characteristics and is a type of a low pass filter. It provides smoothening of image. It removes the noise and more effective at smoothening of images. A one dimensional Gaussian filter has an impulse response, as Eq. (4)[23]:

$$g(x) = \frac{1}{\sqrt{2\pi a}} e^{-ax^2} \quad (4)$$

a : is a variance, x : is the gray level.

the one dimension Gaussian filter as in Eq. (5)[23]:

$$g(x, y) = \frac{1}{\sqrt{2\pi\sigma^2}} e^{-\frac{x^2}{2\sigma^2}} \quad (5)$$

σ : stander deviation, $g(x, y)$: The location of the current pixel.

In two dimension, two Gaussians multiply as in Eq. (6)[23]:

$$g(x, y) = \frac{1}{2\pi\sigma^2} e^{-\frac{x^2+y^2}{2\sigma^2}} \quad (6)$$

σ : stander deviation, $g(x, y)$: The location of this pixel.

Gaussian blur is also known as Gaussian smoothening. This is the result of a Gaussian function in a dark picture. It causes a smooth blur and is used to reduce image noise. The high-frequency components of an image are also reduced and therefore are called low-pass filters[23].

5.3.3 Histogram equalization

The histogram measures the image brightness level and reflects a low or acceptable contrast in the image itself. The histogram with the possible total intensities of L [0, 255] in a digital image as the Eq.(7)[24].

$$h(r_k) = n_k \quad (7)$$

Where n_k is number of pixels with r_k intensity level. It is better working with the normalized histogram that can be obtained by dividing $h(r_k)$ by the total number of pixels in the image, as in Eq.(8)[24]. Any picture histogram is the $P_r(r_k)$ plot against r_k .

$$P(r_k) = \frac{h(r_k)}{\text{numberofrows} * \text{numberofcoloums}} = \frac{n_k}{MN} : \text{for } k=0, 1, 2, \dots (L-1) \quad (8)$$

M: Number of rows. N: Number of columns, L: value of gray level.

HE transformation spreads out the image intensity values along the total range [0, 1] leading to an image with a higher contrast. The HE transformation function is simply the cumulative distribution function (CDF), given in Eq. (9 and 10)[24]:

$$cdf(k) = \sum_{i=0}^k P_r(r_i) : k = 0, 1, 2, \dots L - 1 \quad (9)$$

$$sk = T_{(rk)} = \text{floor} \left[(L - 1) \sum_{i=1}^k P_i \right] = \text{floor} \left[\frac{L-1}{MN} \sum_{i=0}^k n_i \right], k = 0, 1, 2, \dots, (L - 1) \quad (10)$$

Where P_i is pixel intensity, P_r is probability and n_i is number of pixels.

5.4 Segmentation Algorithms

Segmentation of the image is an important processing of images, which seems to be everywhere to look at what is on the picture. Various applications for the segmentation of images are present, for example in the field of filtration of image noise, imagery and the location of objects in satellite images and in automatic transmission control system[25]. In this paper, we used two types of segmentation algorithm: thresholding and region growing.

5.4.1 Thresholding Segmentation

The threshold segmentation is one of the most simple and common methods of image segmentation. It is a common segmentation algorithm that directly divides the processing of the image's gray information based on the gray value of various objectives. Segmentation of thresholds into the methods of local thresholds and global thresholds [26]. Search was made for the optimum method for segmenting kidney stones and can be implement to another part of body tissue like_gallstone. Many types of thresholding were tested and the best result was chosen. In the Otsu method this method depended on the principle of finding the optimal threshold for image segmentation. The threshold is based on the intra or inter-scattering of single pixels on the basis of the Otsu threshold, the entire image is separated by the ideally selected thresholds in the corresponding number of regions.

5.4.2 Region Growing Algorithm

A traditional serial segmentation algorithm is the regional growth method, and its basic idea is to share the similar properties of the pixels in a region. The process requires first a seed pixel to be selected, then the similar pixels to be combined around the pixel in the seed area. As is shown in Figure 10, which illustrates a known regionally growing seed point. . The need to divide the image appears (Figure 10(a)). Two seed pixels are known (marked as gray squares) prepared for regional development. The criterion used was to include the pixel in the region where the pixel of the seed is situated when the absolute gray value difference between the pixels to the seed pixel is regarded as being less than a specific threshold T. As shown in Figure 10(b), which shows the results of T = 3 of re-regional growth and divides the entire plot into two areas. The results of regional growth in T = 6 and the entire plot in an area are illustrated in Figure10(c) [26]. So, it is important to choose a threshold [27].

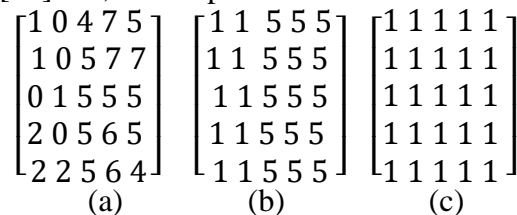


Figure 10: Regional growth examples [26]

6. The Proposed Segmentation Algorithm

The US image is an RGB image. This image is firstly transformed into a gray image. Different noises such as speckling noise and artifacts affect this image. In python, we process this image because it is an open-source python library that is used for image processing tasks. It provides special functionalities that are not provided by other libraries such as filtering, opening, manipulating, and saving images. We have done the median and Gaussian filter preprocessing and have inserted the equalization of the image to improve the quality by increasing image contrast. The process of segmentation uses the threshold and region that grows for the detection of the stone in the images. Steps of the proposed method are described in more details in Algorithm (1).

Algorithm (1): The proposed US segmentation method.

Input: RGB US image with shadowing artifact and speckle noise.

InputImg = cv2.imread (Input).

Step 1: Converting the input image to the grayscale image.

InputImg = cv2.cvtColor (InputImg, cv2.COLOR_BGR2GRAY).

Step 2: Applying median filter to the output of step1.

median = cv2.medianBlur(InputImg, kernel size)

Step 3: Applying Gaussian filter to the output of step2.

Gaussian = cv2.GaussianBlur (median)

Step 4: Applying histogram equalization to the output in step3.

Histogram = cv2.equalizeHist (Gaussian)

Step 5: Take sample thresholding with value 128 to the output of step 4.

cv2.threshold

Step 6: Applying region growing segmentation to the output of step 5.

Let R represents the entire image region. The segmentation process divides R into n sub-regions, R_1, R_2, \dots, R_n , in such a way that.

1. $\cup_i^n R_i = R$, represent initial seed points.
2. R_i is a connected region, $i=1,2,\dots,n$.
3. $R_i \cap R_j = \emptyset$, for all i and j .
4. $P(R_i) = TRUE$, for $i = 1,2 \dots$
5. $P(R_i \cup R_j) = FALSE$.

Where P represent partitions regions.

Output: Segmenting image.

As in shown in Figure 11(a), (b), (c), (d) and (e) Steps of the proposed US segmentation method.

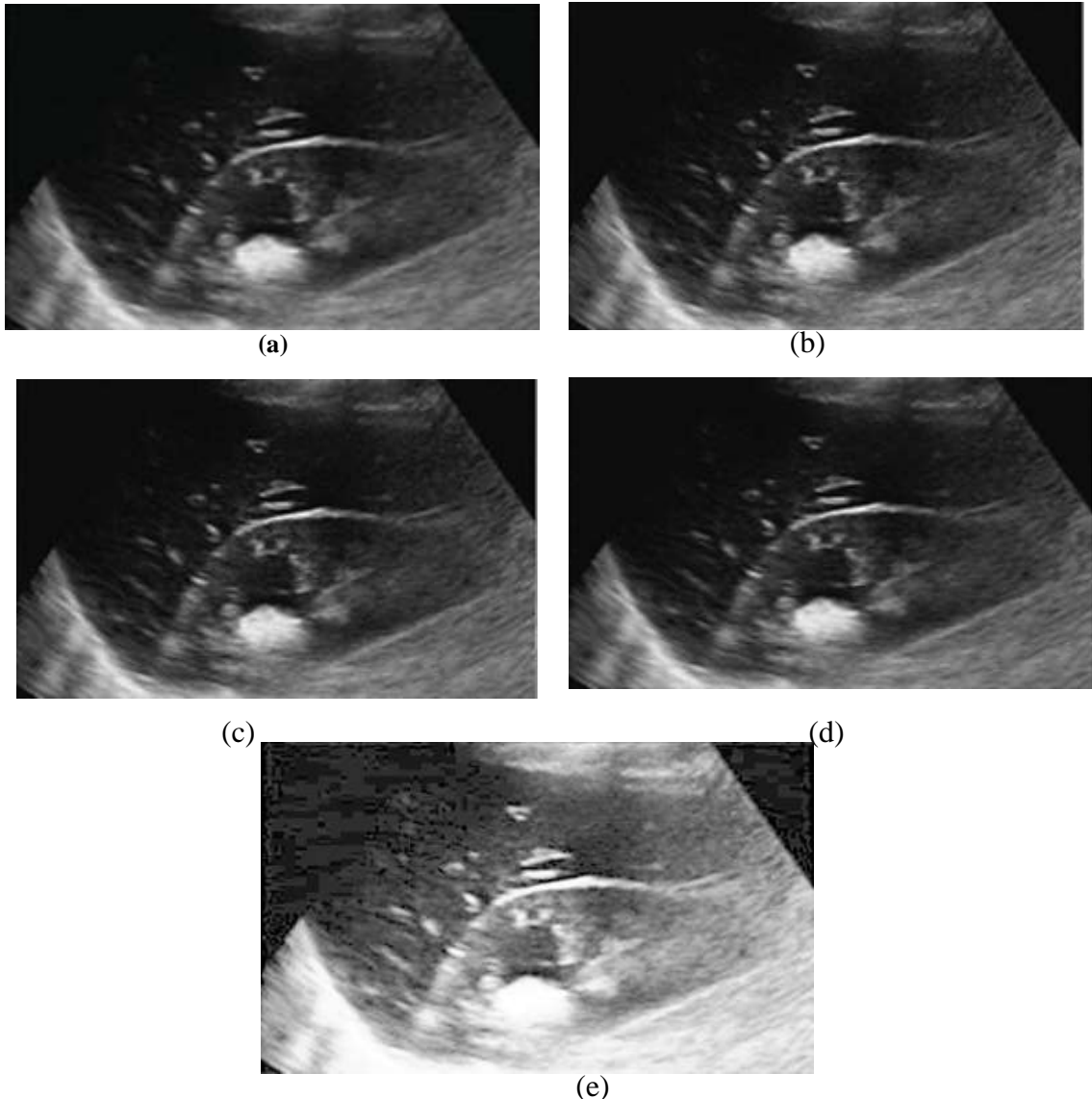


Figure 11: US kidney image, (a) Input image [22] (b) Gray image (c) Image after median filter (d) Image after Gaussian filter (e) Image after histogram equalization

7. Parameter Analysis

We can use several parameters analysis performance to analysis the result of segmentation technique. We used four metrics, mean square error, peak to noise ratio, namely dice coefficient [28] and Jaccard index[29] as parameter analysis.

❖ The Mean Square Error (MSE) is the mean squared error between the filtered image and the original image. MSE can be estimated in one of many ways to quantify the difference between values implied by an estimate and the true quality being certificated. MSE is given by the Eq. (11) below, where M and N is the width and the height of the images. enhanced image I (i, j) and the original image K (i, j). The i and j are the row and column pixels of both the original and enhanced images [30].

$$MSE = \frac{1}{M*N} \sum_{i=0}^{M-1} \sum_{j=0}^{N-1} [I(i,j) - K(i,j)]^2 \quad (11)$$

❖ The Peak Signal to Noise Ratio (PSNR) is the ratio between maximum possible power and corrupting noise that affect representation of image. In other words, PSNR is an engineering term for the ratio between the maximum possible power of a signal and the power of corrupting noise that affects the fidelity of its representation. PSNR is usually expressed as decibel scale. Because many signals have a very wide dynamic range, PSNR is usually expressed in terms of the logarithmic decibel scale and the performance of the proposed algorithms was evaluated in terms of the visual quality and the peak-signal-to-noise-ratio (PSNR). The PSNR is commonly used as measure of quality reconstruction of image as in Eq.(12)[30].

$$PSNR = 20 \log_{10} \left[\frac{(2^n - 1)}{\sqrt{MSE}} \right] [dB] \quad (12)$$

❖ (DC): measures the similarity of two images. The resulting segmented image with the original image that was marked by medical experts was compared with the dice coefficient. It can be calculated by Eq. (13)[22]:

$$DC = \frac{2 * |B1 \cap B2|}{|B1| + |B2|} \quad (13)$$

B1 represents a segmented image in Eq. (13). B2 is the original image before the processing.

❖ Jaccard Index.: In addition, the Jaccard index (JI) is used to identify similarities between two image samples. The ratio of the size of the crossing to the union sample size is defined. The Jaccard index is similar also to the coefficient dice. It is between 0 and 1. The JI value is 1 for the exact same image and 0 for not same. The Eq. (14)[22]:

$$JI = \frac{|B1 \cap B2|}{|B1 \cup B2|} \quad (14)$$

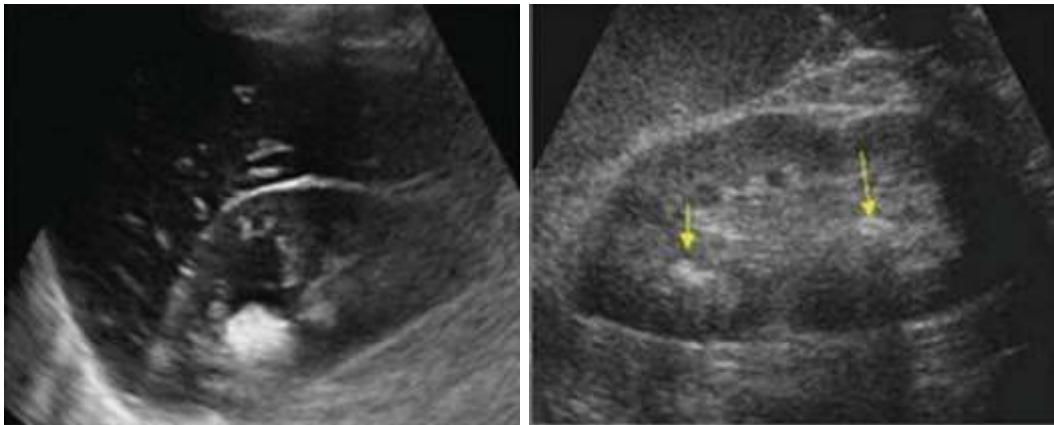
B1 represents a segmented image in Eq. (14). B2 is the original image before processing.

8. Implementation and Results

In this study, the execution was implemented using an Intel core i5 (PyCharm 2020.3.4) using python version 3.8.6. For kidney ultrasound, two samples were used, both have stones. The algorithms involved several steps. The images were loaded in the first step, as in shown in Figure 12(a) and (b) and preprocessing is the next step. The speckle noise removal was performed using median filter and Gaussian filter. In the first stage the median filter was applied. To obtain best result of median filter different values for kernel were examined.

In the second stage the best output of median filter was taken as input to Gaussian filter. In the preprocessing step, the de-speckling image was contrast enhanced with histogram equalization to improve its quality. Processed US images is shown in Figure 13(a) and (b). Quantitative analysis of the preprocessing step was done by using MSE and PSNR illustrated in Table 1 and Table 2. In Table 1 to obtain best values of MSE and PSNR the value kernel of median filter was changed to have minimum MSE reach zero and higher PSNR reach to 361.2019. In Table 2 the experiment result that was obtained when implementing preprocessing method is presented.

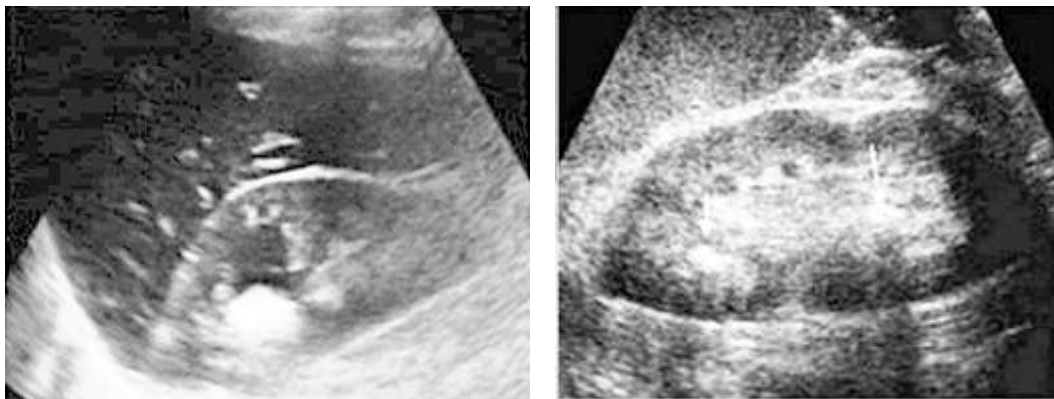
Segmentation of kidney stone US image was carried out using thresholding and region growing methods. Many types of thresholding were experimented with and it was found that 128 manually better as shown in Figure 14(a) and (b). The region growing and thresholding methods were compounded find region of interest (stone) as in shown in Figure 15(a) and (b). Quantitative analysis of segmented image was done using DC and JI. The value of DC and JI illustrated in Table 3. The result of segmentation of kidney stone in US image were promising. The comparison of the results with previous work is presented in Table 4.



(a)

(b)

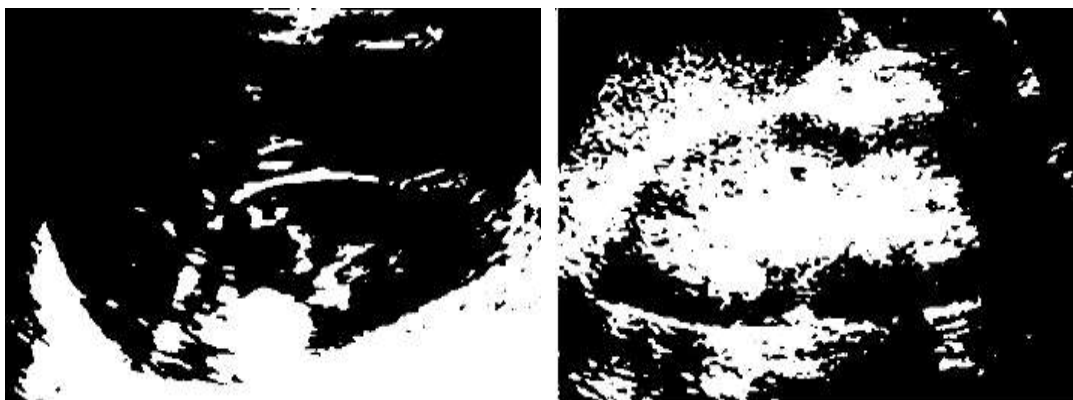
Figure 12: Sample kidney stone US images [22], (a) Sample1 (b) Sample 2



(a)

(b)

Figure 13: Images after preprocessing step, (a) Sample 1 (b) Sample 2



(a)

(b)

Figure 14: Image after thresholding, (a) Sample1 (b) Sample 2

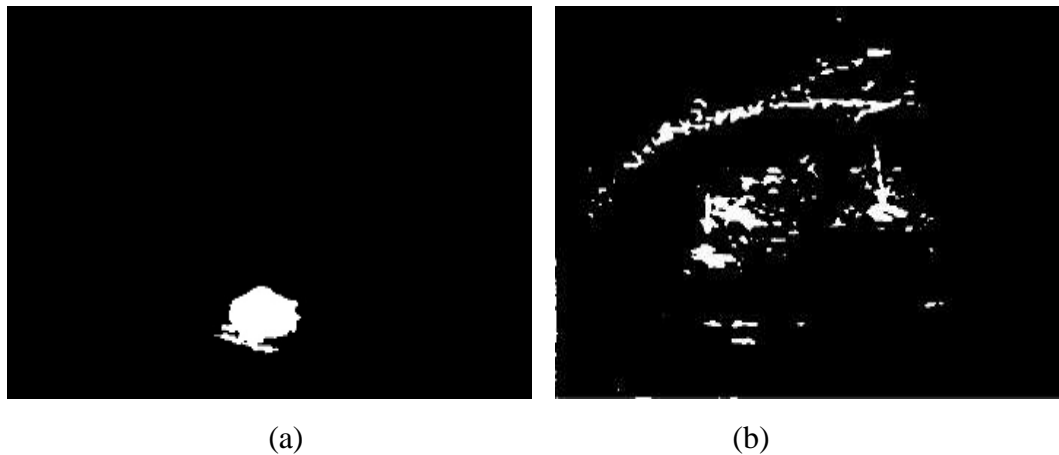


Figure 15: Image after region growing, (a) Sample1 (b) Sample 2.

Table 1: Value of MSE and PSNR for median filter after change kernel

Window size	MSE	PSNR(dB)
3*3	0.0	361.2019
5*5	16.8821	35.8565
9*9	25.7966	34.01516

Table 2: MSE and PSNR of the preprocessing method

Enhancement type	MSE	PSNR(dB)
Median filter	0.0	361.2019
Gaussian filter	0.0	361.2019
Histogram equalization	594.171	20.3916

Table 3: Result of segmented image

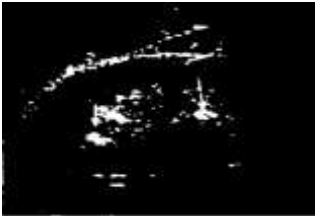
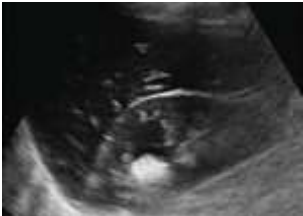
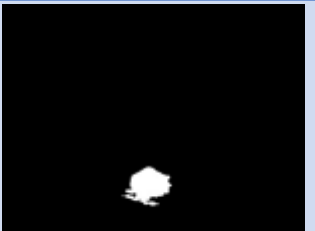
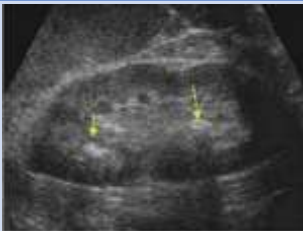

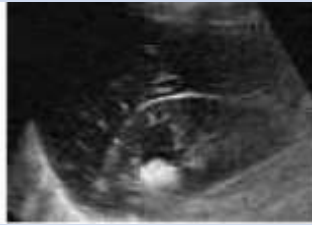
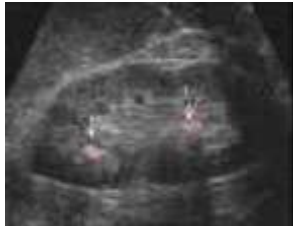
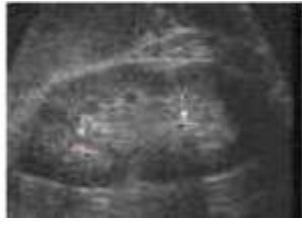
segmented image	Input image	Number of stones	DC	Jl
		1	0.764	0.265
		2	0.804	0.162

Table 4: Result of segmented image for previous work [22]

segmented image	Input image	Number of stones	DC	JI
		1	0.879	0.868
		2	0.825	0.827

9. Conclusions

This paper proposes a method for kidney stone segmentation in US images. Preprocessing is implemented using median filter, Gaussian filter and contrast enhancement using histogram equalization. Thresholding and region growing methods is effectively used to segmenting single as well as multiple stones in US image. Performance of the proposed preprocessing was measured by using MSE and PSNR. Then that performance of segmentation was measured by using DC and JI. The preprocessing and segmentation methods showed the high accuracy of the implemented method. The obtained parameters can help the medical experts in their diagnosis process.

Reference

- [1] M. Antico *et al.*, "Ultrasound guidance in minimally invasive robotic procedures," *Med. Image Anal.*, vol. 54, pp. 149–167, 2019.
- [2] L. Magalhães, S. R. P. Martins, and R. Nogué, "The role of point-of-care ultrasound in the diagnosis and management of necrotizing soft tissue infections," *Ultrasound J.*, vol. 12, no. 1, pp. 10–15, 2020.
- [3] V. Shrimali, R. S. Anand, and V. Kumar, "Comparing the performance of ultrasonic liver image enhancement techniques: A preference study," *IETE J. Res.*, vol. 56, no. 1, pp. 4–10, 2010.
- [4] M. M. Rahman, M. K. PK., A. Aziz, M. G. Arefin, and M. S. Uddin, "Adaptive anisotropic diffusion filter for speckle noise reduction for ultrasound images," *Int. J. Conver. Comput.*, vol. 11, no. 1, pp. 1260-1270, 2013.
- [5] A. I. Nasir, "Artifact in the Image of Ultrasound," *Aust. J. Basic Appl. Sci.*, vol. 12, no. 12, pp. 131–143, 2018.
- [6] S. H. Contreras Ortiz, T. Chiu, and M. D. Fox, "Ultrasound image enhancement: A review," *Biomed. Signal Process. Control*, vol. 7, no. 5, pp. 419–428, 2012.
- [7] P. E. D. J. Huang, J. K. Triedman, N. V. Vasilyev, Y. Suematsu, R. O. Cleveland, "Imaging artifacts of medical instruments in ultrasound-guided intervention," *J. Ultrasound Med.*, vol. 26, pp. 1303–1322, 2007.
- [8] J. A. H. P. C. Tay, S. T. Acton, "A wavelet thresholding method to reduce ultrasound artifacts," *Comput. Med. Imaging Graph.*, vol. 35, pp. 42–50, 2011.
- [9] R. S. W. M. S. Taljanovic, D. M. Melville, L. R. Scalcione, L. H. Gimber, E. J. Lorenz, "Artifacts in musculoskeletal ultrasonography," *Semin. Musculoskelet. Radiol.*, pp. 03–011, 2014.
- [10] M. M. Q. and M. Saric, "Ultrasound imaging artifacts: How to recognize them and how to avoid them," *Echocardiography*, vol. 35, pp. 1388–1401, 2018.

- [11] L. H. G. and M. S. Taljanovic, "Ultrasound Imaging Artifacts," *Springer*, pp. 33–44, 2017.
- [12] D. P. M. Baad, Z. F. Lu, I. Reiser, "Clinical significance of US artifacts," *Radiographics*, vol. 37, pp. 1408-1423, 2017.
- [13] R. G. B. A. Hindi, C. Peterson, "Artifacts in diagnostic ultrasound," *Reports Med. Imaging*, vol. 6, pp. 29–48, 2013.
- [14] M. H. Jang *et al.*, "CCR7 Is Critically Important for Migration of Dendritic Cells in Intestinal Lamina Propria to Mesenteric Lymph Nodes," *J. Immunol.*, vol. 176, no. 2, pp. 803–810, 2006.
- [15] M. A. Yousuf and M. N. Nobl, "A New Method to Remove Noise in Magnetic Resonance and Ultrasound Images," *J. Sci. Res.*, vol. 3, no. 1, pp. 81-89, 2010.
- [16] Sudhamshu Mohan S, Mr. Harsha, and Dr. Padmaja K V, "SVM based Classifier for Noise Classification in Ultrasound B - Mode Images," *Int. J. Eng. Res.*, vol. 05, no. 08, 175-178, 2016.
- [17] N. H. Mahmood, W. Fairuz, J. Wan, and M. Ridzwan, "A User Friendly Guide for Spleen Ultrasound Image Enhancement," vol. 2, no. 2, pp. 248–253, 2012.
- [18] J. C. Dinis, T. F. Moraes, P. H. J. Amorim, O. H. J. Amorim, J. V. L. Silva, and R. B. Ruben, "An open-source GUI application for segment foetal ultrasound images," *Int. J. Signal Imaging Syst. Eng.*, vol. 10, no. 5, pp. 271–277, 2017.
- [19] E. Supriyanto, N. M. Arif, A. H. Rusli, and N. Humaimi, "Semi-automatic thyroid area measurement based on ultrasound image," *Recent Res. Comput. Sci. - Proc. 15th WSEAS Int. Conf. Comput. Part 15th WSEAS CSCC Multiconference*, pp. 228–233, 2011.
- [20] T. Rahman and M. S. Uddin, "Speckle noise reduction and segmentation of kidney regions from ultrasound image," *Int. Conf. Informatics, Electron. Vision, ICIEV 2013*, no.33 ,pp.120-126 2013.
- [21] H. Zhu, J. Sheng, F. Zhang, J. Zhou, and J. Wang, "Improved maximally stable extremal regions based method for the segmentation of ultrasonic liver images," *Multimed. Tools Appl.*, vol. 75, no. 18, pp. 10979–10997, 2016.
- [22] P. T. Akkasaligar, S. Biradar, and S. Badiger, *Segmentation of Kidney Stones in Medical Ultrasound Images*, Springer Singapore, vol. 1036, pp.200-208,2019.
- [23] M. Gupta, H. Taneja, and L. Chand, "Performance Enhancement and Analysis of Filters in Ultrasound Image Denoising," *Procedia Comput. Sci.*, vol. 132, pp. 643–652, 2018.
- [24] N. Salem, H. Malik, and A. Shams, "Medical image enhancement based on histogram algorithms," *Procedia Comput. Sci.*, vol. 163, no.132,pp. 300–311, 2019.
- [25] G. Kaur and S. Jindal, "Region Growing Image Segmentation on Large Datasets Using Gpu," *Int. J. Comput. Technol.*, vol. 15, no. 14, pp. 7486–7497, 2016.
- [26] T. W. Ryan, "Image Segmentation Algorithms," *Archit. Algorithms Digit. Image Process. II*, vol. 0534, pp. 172-180, 1985.
- [27] D. Vilimek *et al.*, "Modeling of Kidney Stones from Ultrasound Images based on Hybrid Regional Segmentation with Active Contours," *Acta Mech. Slovaca*, vol. 23, no. 4, pp. 38–45, 2019.
- [28] J. J. Cerrolaza *et al.*, "Quantification of kidneys from 3D ultrasound in pediatric hydronephrosis," *Proc. Annu. Int. Conf. IEEE Eng. Med. Biol. Soc. EMBS*, vol. 15, pp. 157–160, 2015.
- [29] S. Candemir *et al.*, "Lung segmentation in chest radiographs using anatomical atlases with nonrigid registration," *IEEE Trans. Med. Imaging*, vol. 33, no. 2, pp. 577–590, 2014.
- [30] D. Asamoah, E. Ofori, S. Opoku, and J. Danso, "Measuring the Performance of Image Contrast Enhancement Technique," *Int. J. Comput. Appl.*, vol. 181, no. 22, pp. 6–13, 2018.